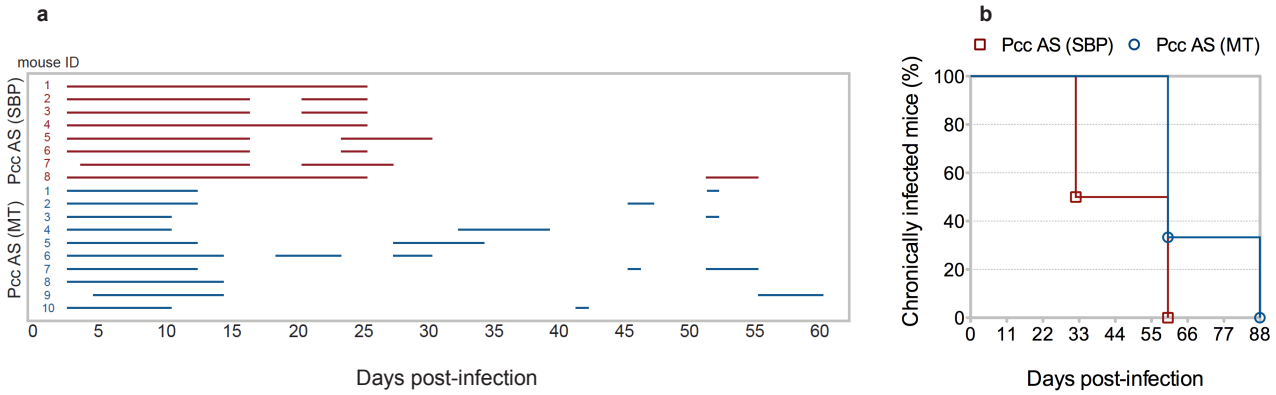

Supplementary Figure 1 | Mosquito transmission of *P.c. chabaudi* AS increases chronicity of infection. **a**, Parasite recrudescences during the chronic phase of infection in C57BL/6 mice injected with 10^5 SBP Pcc AS or infected with Pcc AS via mosquito bite. Solid lines indicate patent parasitaemia. **b**, C57BL/6 mice were injected with 10^5 SBP Pcc AS or infected with Pcc AS via mosquito bite. On days 32, 60 and 88 post-infection, 100 µl blood was isolated from each mouse and injected into a naive RAG KO mouse. Recipient RAG KO mice were monitored for 14 days for the development of patent parasitaemia as a readout of the infection status of each donor C57BL/6 mouse, thereby providing a measure of the chronicity of infection. (n = 8-12 mice per group).

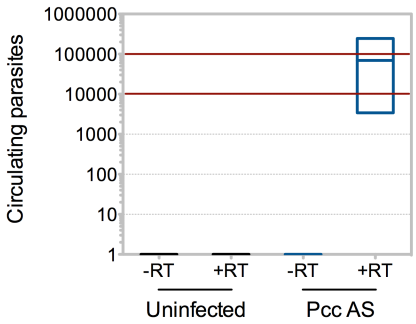

Supplementary Figure 2 | Enumeration of liver merozoite egress. To approximate the number of asexual blood-stage parasites that initiate the erythrocytic cycle in C57BL/6 mice infected with *P.c. chabaudi* AS via mosquito bite, the total number of circulating parasites was enumerated within the first cycle following liver merozoite egress. Parasites were quantified in whole blood by Real-Time PCR, comparing 18S rRNA copy number between samples and a standard curve of pE. Uninfected control mice are shown. Reverse transcription was additionally performed for each sample and standard without Reverse Transcriptase (RT) to confirm the absence of genomic DNA. The red lines define the two parasite doses routinely used to initiate infections via direct injection of infected erythrocytes. (n = 10 mice; data are presented as median with range). Note: The number of asexual blood-stage parasites that initiate the erythrocytic cycle is comparable between mice infected with Pcc AS via injection of infected erythrocytes and mice infected via mosquito bite.

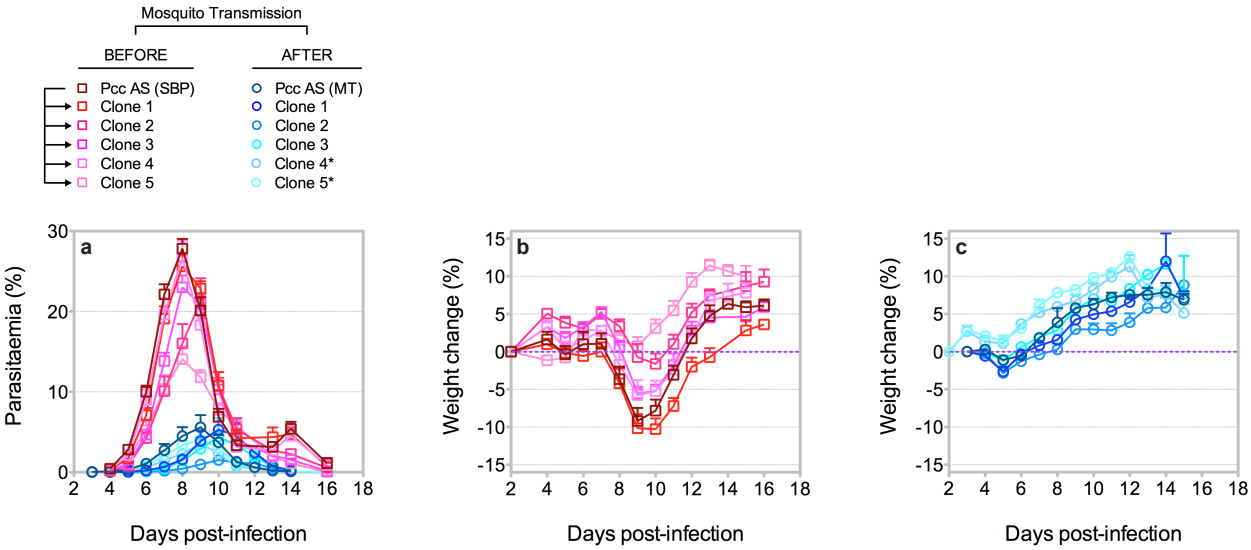

Supplementary Figure 3 | Mosquito transmission of *P.c. chabaudi* AS clones attenuates virulence. *P.c. chabaudi* AS was cloned prior to serial blood passage, and yet may constitute a phenotypically heterogeneous parasite population as a result of continuous passage. Mosquito transmission may therefore select highly transmissible parasites with low virulence; regulation of virulence may therefore be a consequence of parasite selection. To limit parasite heterogeneity, we generated clones of SBP Pcc AS by dilution, and determined their virulence before and after mosquito transmission. **a**-**c**, Parasitaemia (**a**) and weight (**b**-**c**) of C57BL/6 mice injected with 10^5 SBP Pcc AS or 10^5 pE derived from individual clones of SBP Pcc AS, or infected with Pcc AS via mosquito bite or injection of 10^5 pE derived from recently MT lines of Pcc AS (denoted by an asterisk). (n = 6-15 mice per group; data are presented as mean with SEM). Note: All clones of SBP Pcc AS were virulent and transmissible, and mosquito transmission attenuated the virulence of all parasite clones. Vector transmission therefore intrinsically modifies the asexual blood-stage parasite.

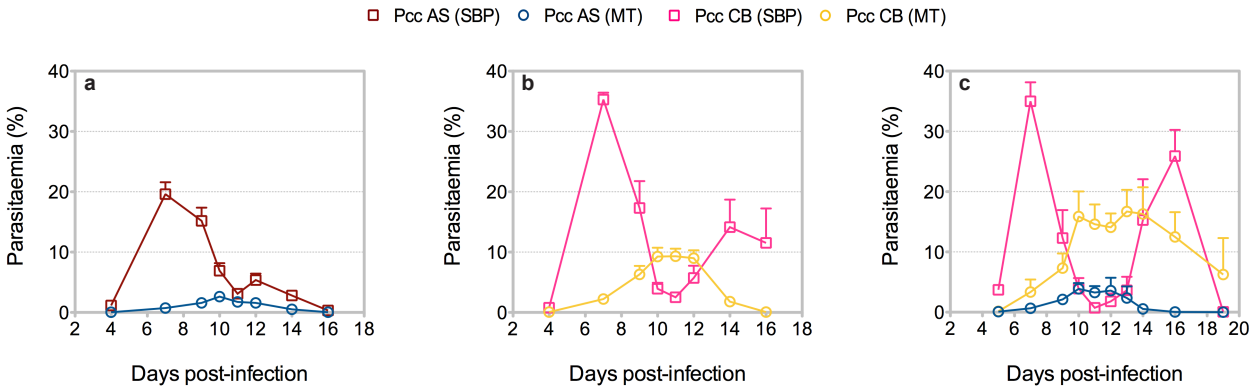

Supplementary Figure 4 | Mosquito transmission of *P.c. chabaudi* CB attenuates virulence. **a**, Parasitaemia of C57BL/6 mice injected with 10^5 SBP Pcc AS or infected with Pcc AS via mosquito bite. **b**, Parasitaemia of C57BL/6 mice injected with 10^5 SBP *P.c. chabaudi* CB (Pcc CB) or infected with Pcc CB via mosquito bite. **c**, Parasitaemia of C57BL/6 mice injected with 10^5 SBP Pcc CB, injected with 10^5 pE derived from a recently MT line of Pcc CB, or injected with 10^5 pE derived from a recently MT line of Pcc AS. (n = 5-20 mice per group; data are presented as mean with SEM). Note: The virulence hierarchy observed between distinct isolates of *P.c. chabaudi* is comparable following mosquito transmission or serial blood passage.

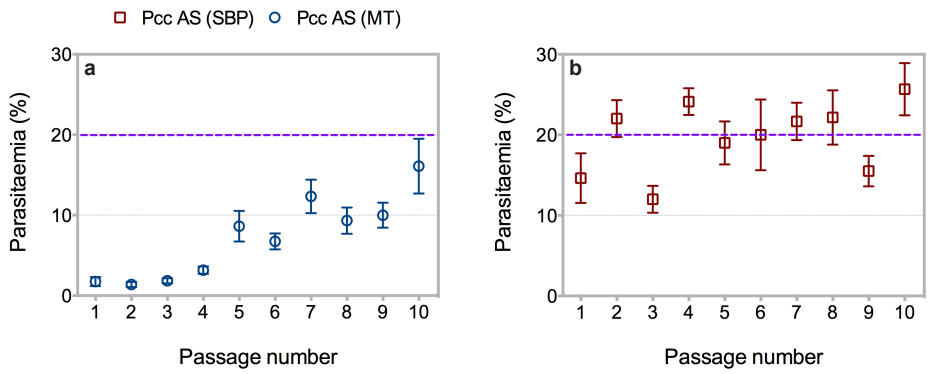

Supplementary Figure 5 | Serial blood passage of mosquito transmitted *P.c. chabaudi* AS rapidly increases parasite growth. **a**-**b**, Serial blood passage of MT Pcc AS (**a**) or SBP Pcc AS (**b**) in C57BL/6 mice. Parasitaemia on day 7 post-infection is shown for each passage. (n = 4-6 mice per group per passage; data are presented as mean with SEM). Note: SBP Pcc AS was not modified further by continued passage, suggesting a parasite intrinsic limit to virulence.

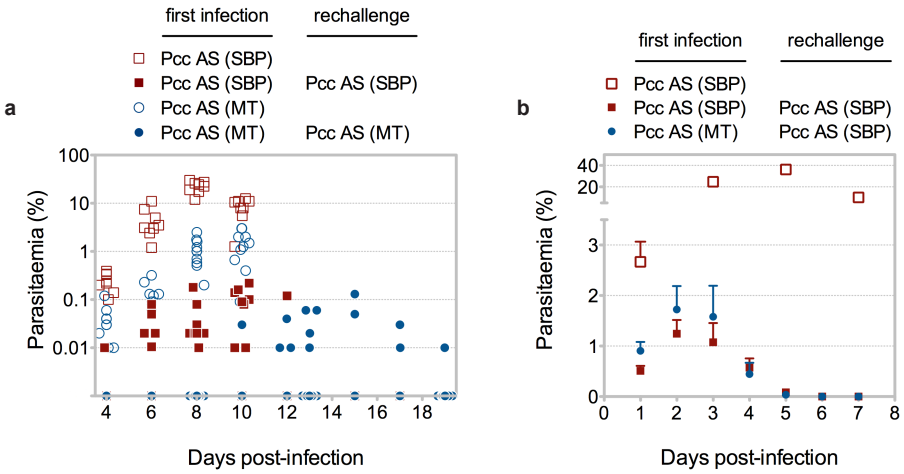

Supplementary Figure 6 | Mosquito transmission of *P.c. chabaudi* AS elicits long-term protection to reinfection. **a**, Parasitaemia of C57BL/6 mice injected with 10^5 SBP Pcc AS or infected with Pcc AS via mosquito bite (open symbols; first four time-points only are shown), or following homologous rechallenge 90 days later (closed symbols). (n = 8-19 mice per group; each individual symbol represents one individual mouse). **b**, Parasitaemia of C57BL/6 mice injected with 10^8 SBP Pcc AS as a first infection (open symbols), or as a homologous rechallenge 90 days after injection with 10^5 SBP Pcc AS or infection with Pcc AS via mosquito bite (closed symbols). (n = 6-10 mice per group; data are presented as mean with SEM).

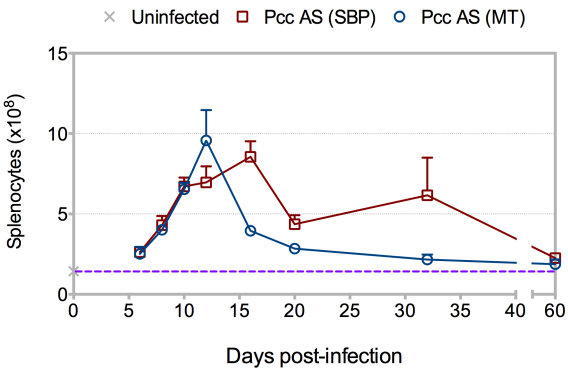

Supplementary Figure 7 | Mosquito transmission of *P.c. chabaudi* AS induces rapid splenomegaly. Number of splenocytes in spleens of C57BL/6 mice injected with 10^5 SBP Pcc AS or infected with Pcc AS via mosquito bite. Uninfected control mice are shown in grey. (n = 5 mice per group per time-point; data are presented as mean with SEM). Note: Splenomegaly peaks and then resolves more rapidly in mice infected via mosquito bite, as compared to mice injected with SBP parasites.

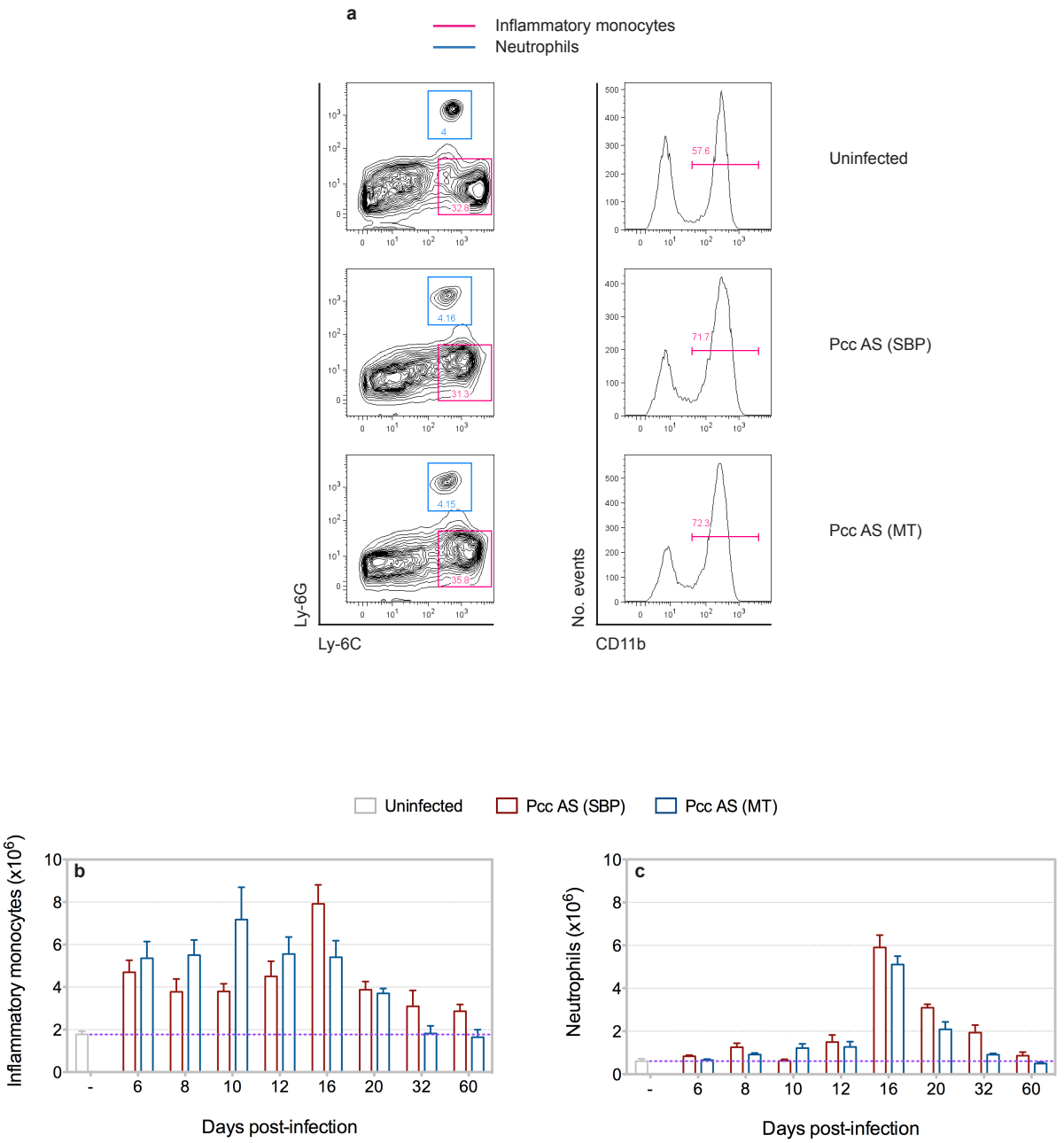

Supplementary Figure 8 | Mosquito transmission of *P.c. chabaudi* AS induces rapid inflammatory cell recruitment to the spleen. **a**, Representative frequencies of inflammatory monocytes (Ly-6C^{HI} Ly-6G^{-} CD11b^{+}) and neutrophils (Ly-6C^{INT} Ly-6G^{HI}) on day 6 post-infection in spleens of C57BL/6 mice injected with 10^5 SBP Pcc AS or infected with Pcc AS via mosquito bite. Uninfected control mice are also represented. Left panels gated on CD3^{-} CD19^{-} NK1.1^{-} Ter-119^{-} splenocytes; right panels gated on CD3^{-} CD19^{-} NK1.1^{-} Ter-119^{-} Ly-6C^{HI} Ly-6G^{-} splenocytes. **b**-**c**, Number of inflammatory monocytes (**b**) and neutrophils (**c**) in spleens of C57BL/6 mice injected with 10^5 SBP Pcc AS or infected with Pcc AS via mosquito bite. Uninfected control mice are shown in grey. (n = 5 mice per group per time-point; data are presented as mean with SEM). Note: Neutrophil expansion follows clearance of peak parasitaemia.

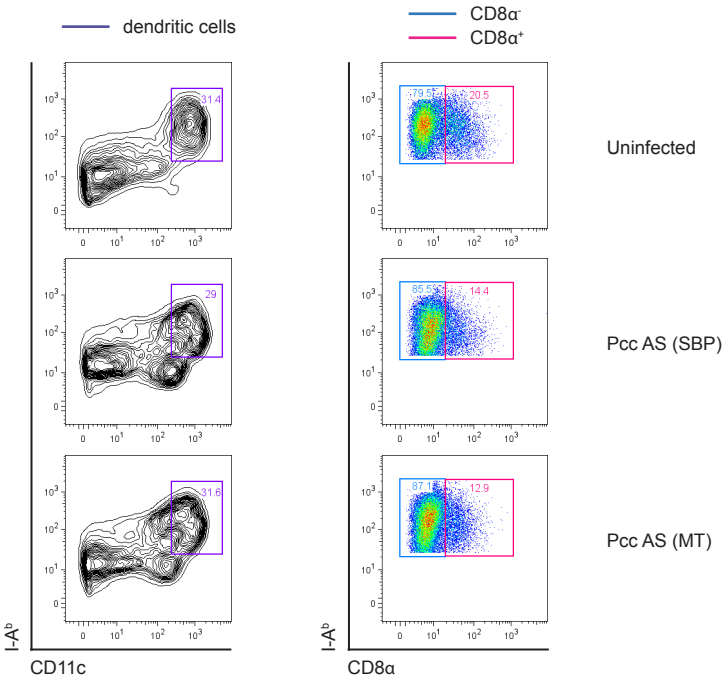

Supplementary Figure 9 | Gating strategy for dendritic cell analysis. Representative frequencies of CD8α^{-} and CD8α^{+} dendritic cells (I-A^{b+} CD11c^{HI}) on day 6 post-infection in spleens of C57BL/6 mice injected with 10^5 SBP Pcc AS or infected with Pcc AS via mosquito bite. Uninfected control mice are also represented. Left panels gated on CD3^{-} CD19^{-} NK1.1^{-} Ter-119^{-} splenocytes; right panels gated on CD3^{-} CD19^{-} NK1.1^{-} Ter-119^{-} I-A^{b+} CD11c^{HI} splenocytes.

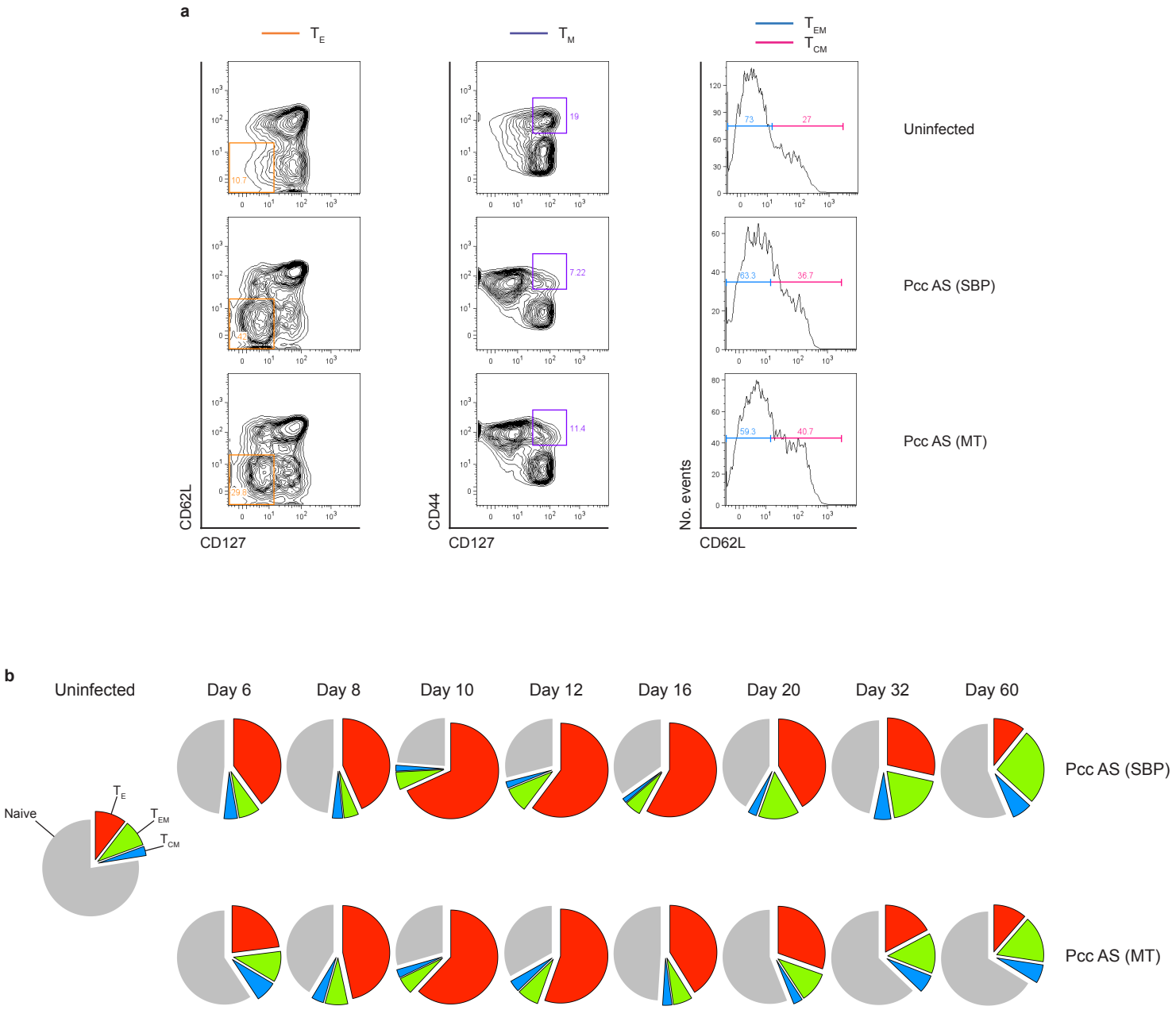

Supplementary Figure 10 | Phenotypic profiling of CD4⁺ T cells. **a**, Representative frequencies of effector CD4⁺ T cells (T_E) (CD62L⁻ CD127⁻), memory CD4⁺ T cells (T_M) (CD44^{HI} CD127⁺), and effector memory (T_{EM}) (CD44^{HI} CD127⁺ CD62L⁻) and central memory (T_{CM}) (CD44^{HI} CD127⁺ CD62L⁺) CD4⁺ T cells on day 6 post-infection in spleens of C57BL/6 mice injected with 10^5 SBP Pcc AS or infected with Pcc AS via mosquito bite. Uninfected control mice are also represented. Left and centre panels gated on CD3⁺ CD4⁺ splenocytes; right panels gated on CD3⁺ CD4⁺ CD44^{HI} CD127⁺ splenocytes. **b**, Frequency of CD4⁺ T cells with a naive, effector, effector memory or central memory phenotype in spleens of C57BL/6 mice injected with 10^5 SBP Pcc AS or infected with Pcc AS via mosquito bite. Uninfected control mice are shown. (n = 5 mice per group per time-point; data are presented as mean frequencies).

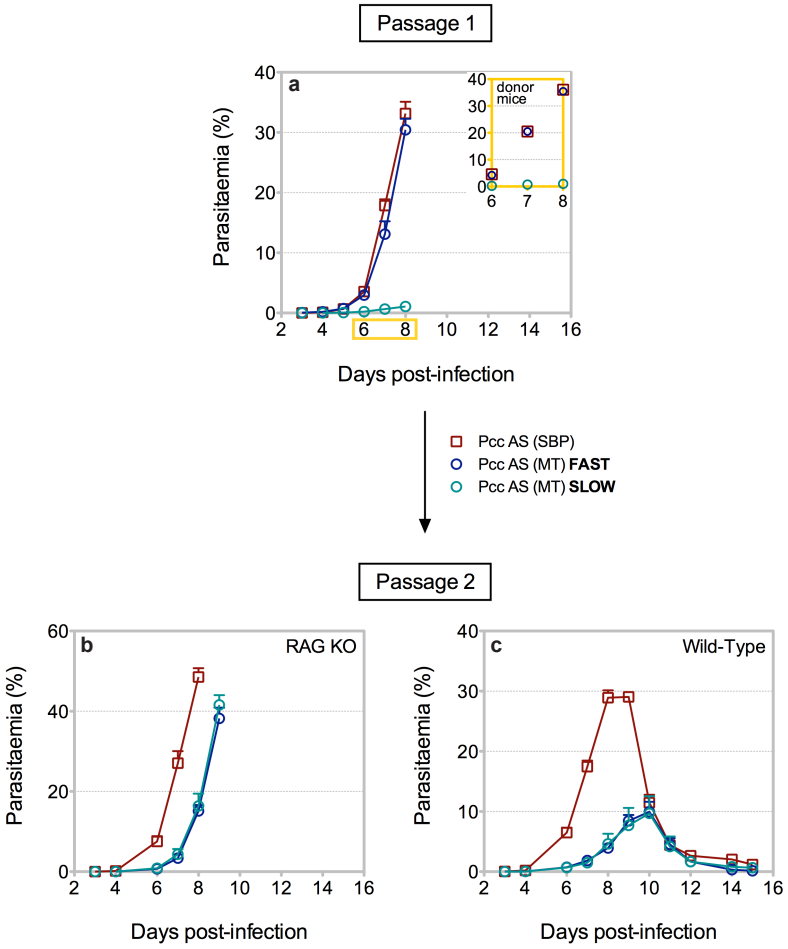

Supplementary Figure 11 | Transformed innate and adaptive immune responses attenuate *P.c. chabaudi* AS virulence independently of parasite growth rate. Serial blood passage may increase the asexual multiplication rate of the blood-stage parasite (ref.[8]). To dissociate immune control of parasite virulence from a potentially modified growth rate, we generated lines of MT *P.c. chabaudi* AS growing at the same rate *in vivo* as SBP parasites. **a**, Parasitaemia of RAG KO mice injected with 10^4 SBP Pcc AS, RAG KO mice injected with 10^5 pE derived from a recently MT line of Pcc AS (generating **FAST**-growing MT Pcc AS), and wild-type mice injected with 10^4 pE derived from a recently MT line of Pcc AS (maintaining **SLOW**-growing MT Pcc AS). Insert shows the growth rate of individual parasite lines isolated at day 7 post-infection to infect naive recipient mice in Passage 2. **b**-**c**, Parasitaemia of RAG KO mice (**b**) and wild-type mice (**c**) injected with 10^4 SBP Pcc AS, 10^4 **FAST**-growing MT Pcc AS or 10^4 **SLOW**-growing MT Pcc AS. (n = 5-10 mice per group; data are presented as mean with SEM). Note: Growth of MT *P.c. chabaudi* AS in immuno-deficient and -sufficient mice was comparably attenuated, as compared to SBP parasites, regardless of whether they were fast or slow growing prior to passage.

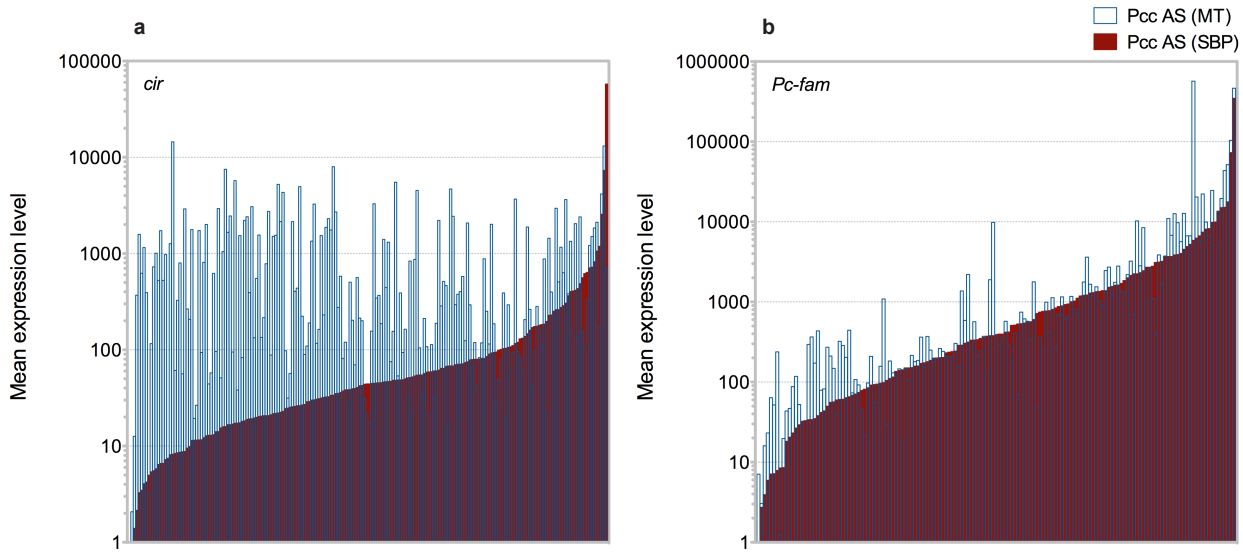

Supplementary Figure 12 | Mosquito transmission of *P.c. chabaudi* AS preferentially regulates expression of the *cir* multi-gene family. **a**-**b**, DESeq-normalised expression levels of 200 *cir* genes (**a**) and 153 *Pc-fam* genes (**b**) in blood-stage parasites following serial blood passage or mosquito transmission. Genes are ranked based on their mean expression level in SBP Pcc AS; the mean expression level of each corresponding gene following mosquito transmission is superimposed. Note: Mosquito transmission revokes the hierarchy of dominant *cir* gene expression that is selected during serial blood passage, but does not substantially modify the ranking of *Pc-fam* gene expression.